Materials Science and Engineering C 58 (2015) 97–102

Contents lists available at ScienceDirect

Materials Science and Engineering C

journal homepage: www.elsevier.com/locate/msec

Direct electrochemistry of hemoglobin and biosensing for hydrogen peroxide using a film containing silver nanoparticles and poly(amidoamine) dendrimer

Marina Baccarin [a,b], Bruno C. Janegitz [b,c,*], Rodrigo Berté [a], Fernando Campanhã Vicentini [b], Craig E. Banks [d], Orlando Fatibello-Filho [b], Valtencir Zucolotto [a]

[a] Nanomedicine and Nanotoxicology Group, Instituto de Física de São Carlos, Universidade de São Paulo, 13566-390 São Carlos, SP, Brazil
[b] Departamento de Química, Universidade Federal de São Carlos, 13565-970 São Carlos, SP, Brazil
[c] Departamento de Ciências da Natureza, Matemática e Educação, Universidade Federal de São Carlos, 13600-970 Araras, SP, Brazil
[d] Faculty of Science and Engineering, School of Chemistry and the Environment, Division of Chemistry and Environmental Science, Manchester Metropolitan University, Chester Street, Manchester M15GD, UK

ARTICLE INFO

Article history:
Received 23 March 2015
Received in revised form 6 August 2015
Accepted 11 August 2015
Available online 12 August 2015

Keywords:
Hemoglobin
Direct electron transfer
Third generation biosensor
Silver nanoparticles
Hydrogen peroxide

ABSTRACT

A new architecture for a biosensor is proposed using a glassy carbon electrode (GCE) modified with hemoglobin (Hb) and silver nanoparticles (AgNPs) encapsulated in poly(amidoamine) dendrimer (PAMAM). The biosensors were characterized using ultraviolet–visible spectroscopy, ζ-potential and cyclic voltammetry to investigate the interactions between Hb, AgNPs and the PAMAM film. The biosensor exhibited a well-defined cathodic peak attributed to reduction of the Fe^{3+} present in the heme group in Hb, as revealed by cyclic voltammetry in the presence of O_2. An apparent heterogeneous electron transfer rate of 4.1 s^{-1} was obtained. The Hb–AgNPs-PAMAM/GCE third generation biosensor was applied in the amperometric determination of hydrogen peroxide over the linear range from 6.0×10^{-6} to 9.1×10^{-5} mol L^{-1} with a detection limit of 4.9×10^{-6} mol L^{-1}. The proposed method can be extended to immobilize and evaluate the direct electron transfer of other redox enzymes.

© 2015 Elsevier B.V. All rights reserved.

1. Introduction

Hemoglobin (Hb) is a metalloprotein with a quaternary structure that contains four polypeptide chains (globin chains) and one heme group bound to each of the globin chains. It is present in red blood cells and has utmost importance to humans, since it carries oxygen throughout the body via the circulatory system [1]. Hb presents a metal cation (iron) bound to the porphyrin and due to its reported beneficial properties, efforts have been conducted to develop biosensors using Hb for the determination of hydrogen peroxide (H_2O_2) [1,2]. In this regard, third-generation biosensors based on Hb and direct electron transfer between the redox couple of the active center of the biomolecule and the electrode surface have been proposed. Such biosensors offer advantages such as high sensitivity and selectivity as they operate closer to the potential of the enzyme, and therefore reducing the signal from interfering reactions/species [3–5].

Nanomaterials present distinct characteristics, such as good mechanical strength and high electrical conductivity [6], which have attracted great interest to the scientific community [7]. Such properties combined with the potential applications of nanotechnology have made such materials very attractive for the development of electrochemical sensors [8–12] and biosensors [13–16]. Indeed, stable dispersions have been prepared with nanomaterials for electroanalysis [17,18], which provide good stability and do not interfere in the electron transfer at electrode/solution interface. As examples, we can highlight the use of metal nanoparticles (MNPs) [18–21], graphene [2,22] and/or carbon nanotubes [23,24].

Modified electrodes with MNPs such as gold, silver, palladium, copper and nickel nanoparticles present advantages over the use of macroelectrodes, including the larger contact area, increased mass transfer and electrocatalysis [25]. Silver nanoparticles (AgNPs) are used in the manufacture of consumer products, such as textiles, personal hygiene, food storage containers, appliances, paint and even dietary supplements due to their antimicrobial effects [26]. Moreover, AgNPs have been used in the development of new electrochemical sensors and biosensors [27–29].

Dendrimers are macromolecules with high molecular weight synthesized by sequentially radial growth from a polyfunctional core. The number of monomer units incorporated into each layer is, successively, doubled or tripled compared to the previous layer. As a result, a highly branched structure is created with a large number of functional groups on its surface, e.g. poly(propyleneimine) and poly(amidoamine)

* Corresponding author at: Departamento de Ciências da Natureza, Matemática e Educação, Universidade Federal de São Carlos, 13600-970 Araras, SP, Brazil.
E-mail address: brunocj@ymail.com (B.C. Janegitz).

http://dx.doi.org/10.1016/j.msec.2015.08.013
0928-4931/© 2015 Elsevier B.V. All rights reserved.

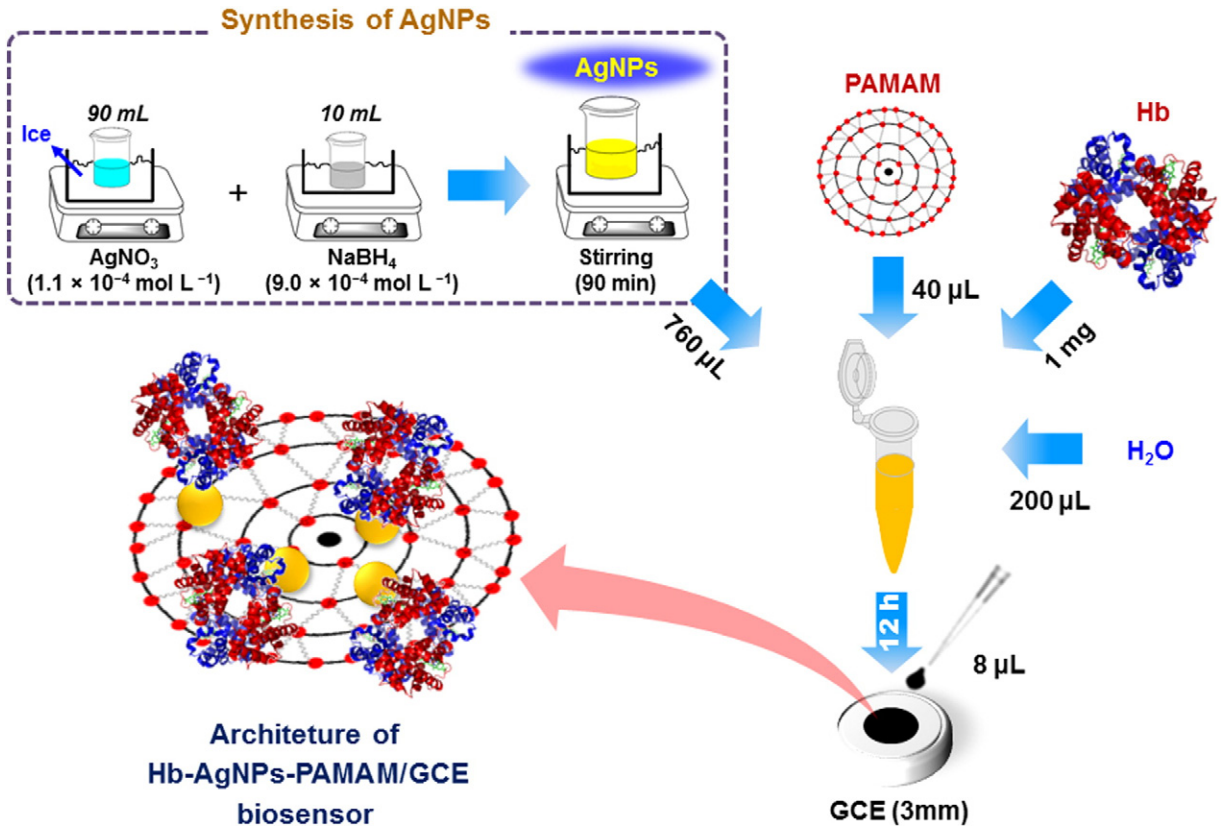

Fig. 1. Schematic representation of Hb–AgNPs-PAMAM/GCE biosensor fabrication process.

(PAMAM). PAMAM is a dendrimer consisting of alkyl diamine core and branches of tertiary amines, which are applied in different areas such as medicine, genetics, biotechnology and cosmetics [30,31]. PAMAM can be used for immobilization of biological materials through covalent and/or electrostatic bonds between their amino/hydroxyl groups and peripheral amine groups in the enzyme.

Herein, we report a new architecture for the fabrication of third-generation biosensors using Hb, AgNPs and PAMAM immobilized on the surface of glassy carbon electrode (Hb–AgNPs–PAMAM/GCE), resulting in a device easy to construct, that exhibits fast response and high sensitivity and can be applied to the determination of H_2O_2.

2. Experimental

2.1. Chemicals

Silver nitrate, sodium borohydride, PAMAM and bovine Hb were obtained from Sigma-Aldrich. All other reagents were of analytical grade and were used as received. All solutions were prepared with ultrapure water (resistivity > 18.0 MΩ cm) obtained from a Millipore Milli-Q system (Billerica, USA). A 0.1 mol L^{-1} of phosphate buffer (pH 7.0) was used as the electrolyte solution, which was prepared with Na_2HPO_4 and NaH_2PO_4 salts from Sigma-Aldrich.

2.2. Instruments

Scanning electron microscopy (SEM) images were obtained with a Supra 35-VP microscope (Carl Zeiss, Germany), with an electron beam energy of 25 keV. Histogram was constructed using the public-domain Image J image-processing software. A Hitachi U2001 spectrometer was used for measurements of UV–vis spectroscopy and a Zetasizer Nano ZS (Malvern) was employed to investigate the interactions between Hb, the AgNPs and PAMAM. Electrochemical measurements were performed using an Autolab PGSTAT12 (Eco Chemie) potentiostat/galvanostat coupled to a microcomputer managed by 4.9 GPES software. A conventional three-electrode system, using the biosensor Hb–AgNPs–PAMAM/GCE as a working electrode, a platinum plate as a counter electrode, and a Ag/AgCl (3.0 mol L^{-1} KCl) as a reference electrode completing the circuit was employed for electrochemical studies.

2.3. Synthesis of silver nanoparticles

An aliquot of 90 mL of 1.1×10^{-4} mol L^{-1} $AgNO_3$ stock solution and 10 mL of 9.0×10^{-4} mol L^{-1} $NaBH_4$ solutions was respectively transferred in two flasks. Each solution was stirred individually for 20 min in an ice bath. The solutions were mixed to obtain a final concentration of 9.9×10^{-5} mol L^{-1} $AgNO_3$ and 9.0×10^{-5} mol L^{-1} of $NaBH_4$. This mixture was stirred for 90 min in an ice bath. The final product (AgNPs), a yellow solution, was stored in an amber vial, protected from light, at room temperature for further use. The formation of AgNPs was confirmed by UV–vis spectrometry. For this, 100 µL of stock solution was diluted in water (1.0 mL) and the sample was analyzed.

2.4. Preparation of Hb–AgNPs-PAMAM/GCE biosensor

The GCE (Ø = 3.0 mm) was polished with alumina for 5 min to obtain a mirror-like surface on the electrode and then washed with ultrapure water. A mass of 1.0 mg of Hb was dispersed in 760 µL AgNP solution. Following, 40 µL of a 6.6×10^{-2} mol L^{-1} PAMAM and 200 µL of ultrapure water were added to this suspension. The resultant mixture was stirred for 30 min for homogenization. Next, 8 µL of the Hb–AgNPs-PAMAM dispersion was dropped onto the GCE surface and the solvent was evaporated at 4 °C in a desiccator for 12 h. For comparison,

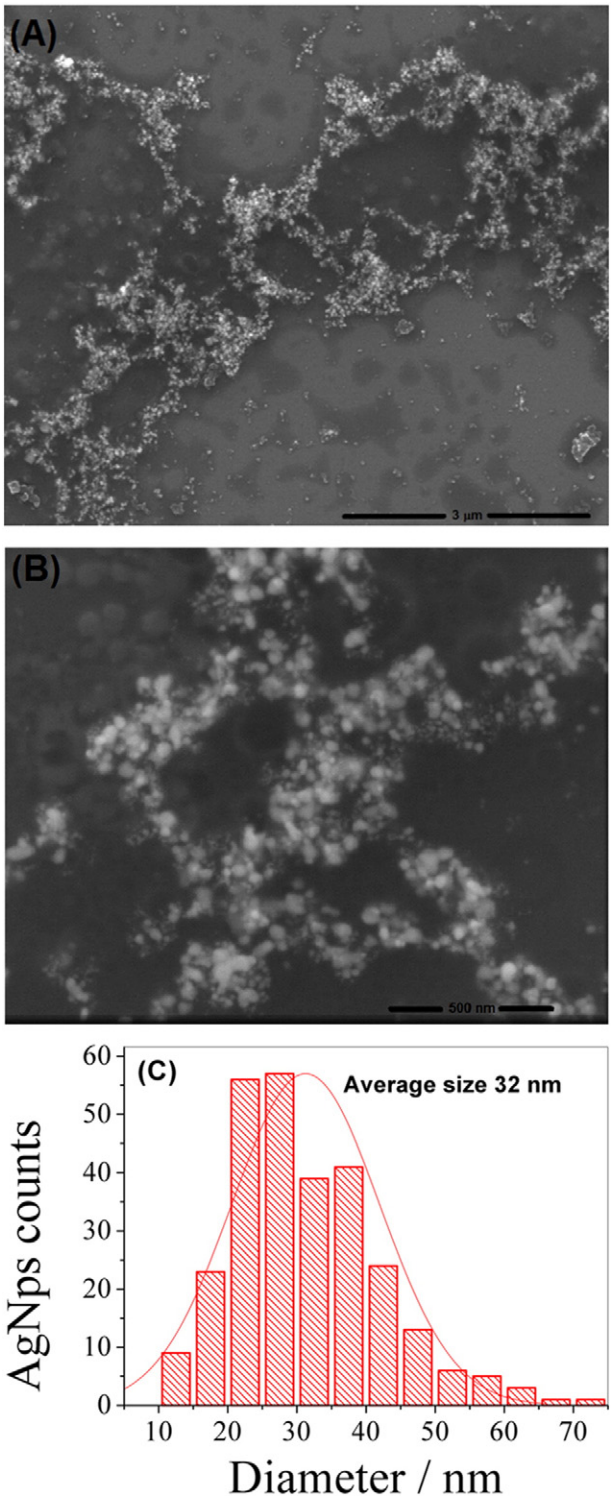

Fig. 2. SEM images of AgNPs and (A and B). Histogram of the AgNPs size distribution (C). The solid line corresponds to a Gaussian fit.

AgNPs–PAMAM/GCE and Hb–PAMAM/GCE were prepared to compare the ability to detect H_2O_2. When it was not in use, the electrode was stored in a refrigerator under the same conditions mentioned above. The proposed biosensor was designated as Hb–AgNPs-PAMAM/GCE and its schematic fabrication is presented in Fig. 1.

To confirm the interaction between the compounds of film Hb–AgNPs–PAMAM, UV–vis spectrometry measurements were performed.

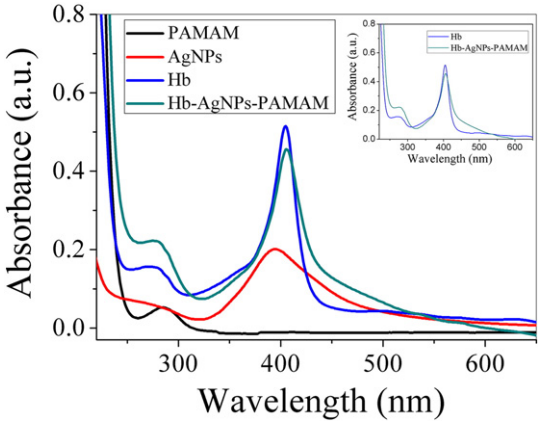

Fig. 3. Hb, PAMAM and AgNPs Hb–AgNPs-PAMAM UV–vis spectra. Hb and Hb–AgNPs-PAMAM spectra (inset).

Thus, 100 μL of stock solution was diluted in water (1.0 mL) and absorbance spectrum of the film was observed.

3. Results and discussion

3.1. Characterization of the Hb–AgNPs-PAMAM composites

Fig. 2a and b shows a typical SEM image of the obtained AgNPs. Then, it was constructed a histogram of the AgNP diameters which presented an average diameter estimated at 32 nm (Fig. 2c). The interaction between Hb, PAMAM and AgNPs was investigated by UV–vis spectroscopy, and Fig. 3 depicts the spectra of each individual system. It can be seen that both Hb and AgNPs absorb in the region from ca. 350 to ca. 500 nm. Therefore, no significant difference was observed in the spectra, once both present the absorption in the same region. PAMAM does not absorb in the visible region (350–700 nm). In addition, a maximum in the absorbance at ca. 400 nm is observed, corresponding to the absorption of the Hb and Hb–AgNPs–PAMAM (Fig. 3, inset). The position of the Soret absorption band from the heme group may indicate a possible denaturation of heme protein [32]. If the Hb molecule denatures, the Soret band shifts, or disappears. However, it can be seen that the Hb molecule absorbs in the same region in both spectra (Fig. 3 and Fig. inset) which indicate that the Hb in Hb–AgNPs–PAMAM did not denature, which is a good indicative that the protein preserved its biological activity [1,33,34].

The behavior and dispersion stability of the Hb–AgNPs–PAMAM were investigated. According to the literature, the suspension stability can be affected by changes in pH and/or ionic strength. Furthermore, the higher the value of the zeta potential (in modulus), the higher the

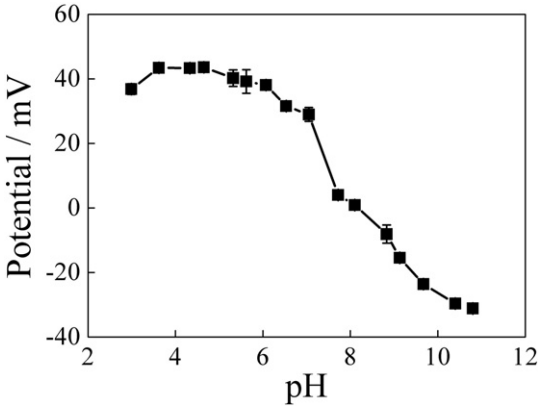

Fig. 4. ζ-Potential dependence of Hb–AgNPs–PAMAM vs. pH solution.

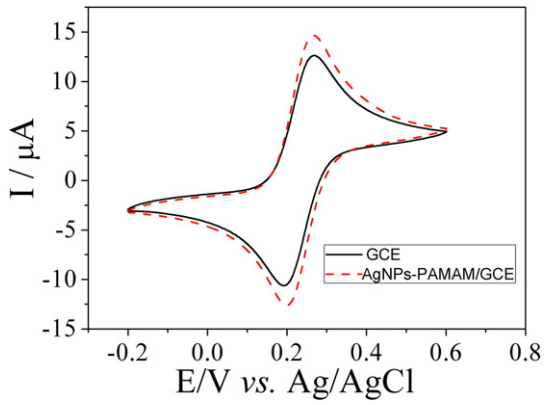

Fig. 5. Cyclic voltammograms (100 mV s^{-1}) for 1.0 mmol L^{-1} $[Fe(CN)_6]^{4-}$ in 1.0 mol L^{-1} KNO_3 obtained with GCE (solid line) and AgNPs–PAMAM/GCE (dashed line).

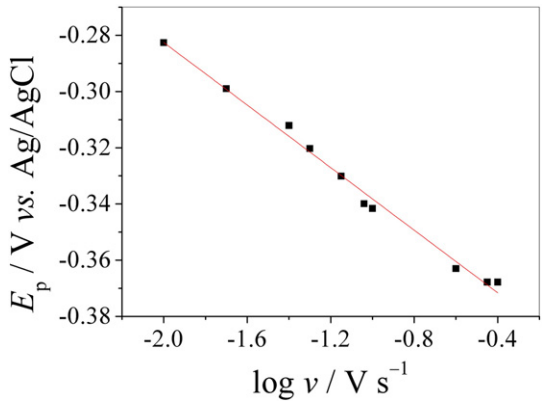

Fig. 7. Cathodic peak potentials (E_{pc}) versus the logarithm of the potential scan rate (log v) obtained using the Hb–AgNPs–PAMAM/GCE.

stability of the dispersion [35]. As shown in Fig. 4, the Hb–AgNPs–PAMAM presents positive zeta potential values in the pH range between 3.0 and 7.7. For pH values higher than 7.7 the ζ-Potential is negative and decreases significantly. A probable explanation for this fact is related to the pK_a of hemoglobin, which is equal to 7.1 [36]; the more acidic the environment, the more protonated is Hb, denoting the interaction between the protein and the AgNPs.

3.2. Electroactive area of GCE and AgNPs–PAMAM/GCE

The electroactive area of the GCE and AgNPs–PAMAM/GCE was estimated using cyclic voltammetry at different scan rates, using 1.0 mmol L^{-1} $[Fe(CN)_6]^{4-}$ in 1.0 mol L^{-1} KNO_3 solution via the Randles–Sevcik equation for an electrochemical reversible process, as represented below (Eq. (1)) [37].

$$Ip = 2.69 \times 10^5 A\, C\, D^{1/2}\, n^{3/2}\, v^{1/2} \quad (1)$$

where I_p is the peak current (A), A is the electroactive area (cm^2), C is the concentration of $[Fe(CN)_6]^{4-}$ solution (mol cm^{-3}), D (6.2×10^{-6} cm^2 s^{-1}) is the diffusion coefficient of the molecule in solution (cm^2 s^{-1}), n is the number of electrons involved in the redox reaction and v is the potential scan rate (V s^{-1}).

Cyclic voltammograms for AgNPs–PAMAM/GCE and GCE were obtained for a 1.0 mmol L^{-1} $[Fe(CN)_6]^{-4}$ in the 1.0 mol L^{-1} KNO_3 solution for scan rates ranging from 10 to 400 mV s^{-1}. The obtained values were 0.060 cm^2 for GCE and 0.092 cm^2 for AgNPs–PAMAM/GCE. Fig. 5 presents the cyclic voltammograms at 100 mV s^{-1} for 1.0 mmol L^{-1} $[Fe(CN)_6]^{4-}$ in 1.0 mol L^{-1} KNO_3 obtained with a GCE (solid line) and AgNPs–PAMAM/GCE (dashed line). The presence of AgNPs promoted an increase in the electroactive area if compared to the GCE which is in agreement with previous studies [29,38].

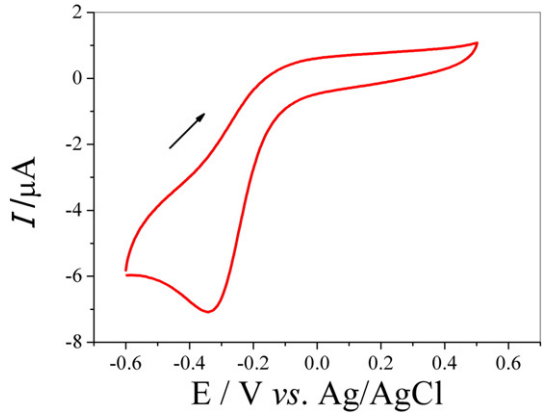

Fig. 6. Cyclic voltammogram obtained using Hb–AgNPs–PAMAM/GCE in 0.1 mol L^{-1} phosphate buffer solution (pH 7.0) at a scan rate of 100 mV s^{-1}.

3.3. Electrochemical behavior of the biosensor

The electrochemical behavior of the Hb–AgNPs–PAMAM/GCE was investigated in a solution of 0.1 mol L^{-1} phosphate buffer (pH 7.0) at a scan rate of 100 mV s^{-1}. As can be seen from Fig. 6, a well-defined reduction peak was observed for Hb–AgNPs–PAMAM on the cathodic scan (at −0.33 V). However, no corresponding oxidation peak was detected. This peak is related with the reduction peak of Fe^{3+} present in the heme group of hemoglobin. In addition, the cyclic voltammogram does not display the typical non-catalytic profile of Hb that can be observed in previous works [1,2]. Instead, we can observe a sigmoidal shape. Probably, because the electrolyte solution was not deaerated before running the experiments, the voltammogram shape reflects some influence of response of Hb towards oxygen instead of the non-catalytic electrochemical response of Hb. The same behavior has been observed in other hemoglobin biosensors performed in the presence of O_2 [39–41].

The effect of scan rate upon the voltammetric response of the Hb–AgNPs–PAMAM/GCE was explored. It was observed that the current cathodic peaks were linearly proportional to the scan rate from 10 to 400 mV s^{-1}, with the linear regression equation $E_{pc} = -0.39 - 0.056$ log v (V s^{-1}) (Fig. 7). Using the Laviron [42] Eq. (2) for a totally irreversible wave, E_{pc} as a function of logarithm of the potential scan rate (log v),

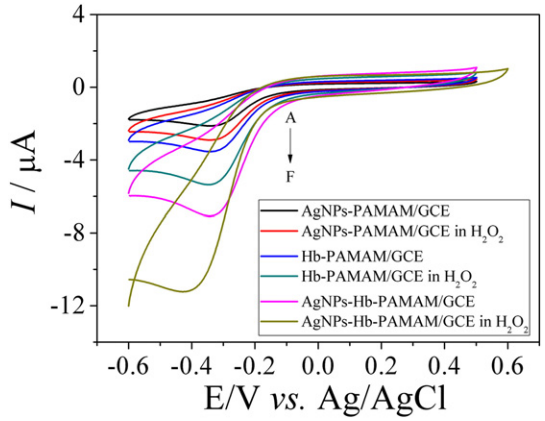

Fig. 8. Cyclic voltammograms obtained using AgNPs–PAMAM/GCE (A and B) Hb–PAMAM/GCE (C and D) and Hb–AgNPs–PAMAM/GCE (E and F) in 0.1 mol L^{-1} phosphate buffer solution (pH 7.0) (A and C) in the absence and in the presence of 1.0×10^{-5} mol L^{-1} H_2O_2 (B and D) at a scan rate of 100 mV s^{-1}.

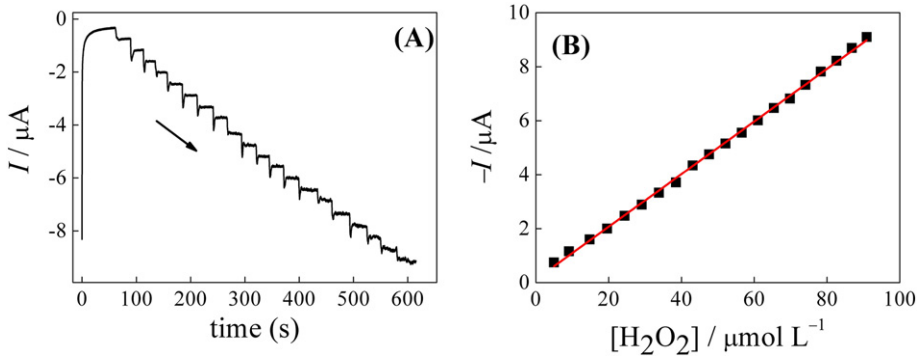

Fig. 9. (A) Amperogram obtained using Hb–AgNPs-PAMAM/GCE biosensor in the presence of different concentrations of H_2O_2 (1 to 20). Successive addition of 30 μL of H_2O_2 in 0.1 mol L^{-1} phosphate buffer solution (pH 7.0), applied potential of −400 mV; and (B) analytical curve.

it was possible to obtain information such as charge transfer coefficient (α) and heterogeneous electron transfer rate constant (k_s).

$$E_{pc} = E^{\circ} - \frac{2.3\,R\,T}{\alpha\,n\,F}\left[\log\frac{\alpha\,n\,F}{R\,T\,k_s} + \log v\right] \quad (2)$$

where E_{pc} is the cathodic peak potential, n is the number of electrons and R, F, and T have their usual meanings. Using the slope of the plot of cathodic peak potential versus log v (Fig. 7) the values in Eq. (2) were replaced. In accordance with the cathodic process, the relationship αn was estimated to be 1.06 and the number of electrons (n) transferred in the reduction of Hb is 1, due the species of Fe^{3+} reduction to Fe^{2+} of the heme iron in Hb. Thus, the value for α was calculated to be approximately 1.06. In addition, by using the linear coefficient of the plot E_{pc} versus log v the estimated k_s value was 4.1 s^{-1}. This value is 5.6 times higher than previous reports by Sun and coworkers [1] and 29.4 times higher than that calculated by Feng and coworkers [43], which demonstrates the ability of the proposed biosensor in promoting the electron transfer between the Hb and the electrode surface.

3.4. Determination of H_2O_2

The decomposition of hydrogen peroxide is an important biological process [44]. This substance is strongly oxidizing and can be harmful to cells. It is present in some biological reactions as the main product of various oxidase enzymes, e.g., the oxidation reaction of glucose by molecular oxygen catalyzed by glucose oxidase, generating products such as gluconic acid and H_2O_2 [45]. Therefore, it is important to quantify this molecule in several processes [46]. Voltammetric responses of the AgNPs–PAMAM/GCE, Hb–PAMAM/GCE and Hb–AgNPs–PAMAM/GCE were explored in a 0.1 mol L^{-1} phosphate buffer solution in the absence and presence of 1.0×10^{-6} mol L^{-1} H_2O_2 at a scan rate of 100 mV s^{-1} (Fig. 8). We can observe that all electrodes presented similar voltammetric profile and the results showed an increase of the cathodic peak current in the presence of H_2O_2, related to the catalytic reduction of the analyte of interest in aired solution. However, AgNPs–PAMAM/GCE presented lower reduction peak related to the reduction of Ag^+ to Ag. In addition, we can affirm that the use of Hb and AgNPs together improves the catalysis of the reduction process of the H_2O_2 (Hb–AgNPs–PAMAM/GCE). In the literature a biosensor containing AgNPs and Hb presented the similar behavior. Tian et al. [47] developed a biosensor for H_2O_2 with Hb, AgNPs, and chitosan. In this work it was possible to observe that AgNPs provided the Hb molecules effective adsorption sites that their active centers can be easily accessed. In this way, the electron transfer between Hb and the electrode surface is significantly promoted. Therefore, it is clear that AgNPs increase the electroactive area and improve the catalysis of the reduction process of the H_2O_2 performed by the heme group of the Hb.

Subsequently, amperometric measurements were recorded using Hb–AgNPs–PAMAM/GCE at a stirring of 900 rpm in 0.1 mol L^{-1} phosphate buffer solution (pH 7.0) in the presence of different concentrations of H_2O_2 by applying a reduction potential of −400 mV. The biosensor displayed increasing amperometric response proportional to the H_2O_2 concentration, as shown in Fig. 9A. The calibration curve showed a linear range for H_2O_2 solution from 6.0×10^{-6} to 9.1×10^{-5} mol L^{-1} following the equation I_p (μA) = $-1.196 \times 10^{-7} - 0.0975$ [H_2O_2] (μmol L^{-1}), with a correlation coefficient of 0.998 (Fig. 9B). The proposed biosensor presented a detection limit of 4.9×10^{-6} mol L^{-1} calculated by the relationship: 3 × SD/S, where SD is the standard deviation of ten blank (electrolyte only) measurements and S is the slope of the analytical curve.

Long-term stability of the proposed biosensor was evaluated by monitoring the response in the presence of 1.0×10^{-6} mol L^{-1} H_2O_2 in 0.1 mol L^{-1} phosphate buffer solution (pH 7.0) during one month (90 determinations in this period). The analytical signal decreased 5.9% after this time. Moreover, the repeatability of one Hb–AgNPs–PAMAM/GCE biosensor was evaluated for a 4.0×10^{-6} mol L^{-1} H_2O_2 in 0.1 mol L^{-1} phosphate buffer solution (pH 7.0). Relative standard deviation (RSD) obtained for intra-day repeatability (n = 10) was 4.1% and inter-day repeatability (n = 3) was 5.4%, indicating a good stability of the biosensor.

Interference of species such as cysteine, L-ascorbate, and glucose in the detection of H_2O_2 was studied by amperometry in the presence of 1.0×10^{-6} mol L^{-1} H_2O_2 solution spiked with a 100-fold excess of interfering species. The evaluated species presented less than 5% change in the analytical response. Therefore, at the concentration evaluated they do not affect the determination of H_2O_2 by performing Hb–AgNPs-PAMAM/GCE biosensor.

Hb–AgNPs-PAMAM/GCE biosensor was applied to the detection of the H_2O_2 in synthetic human serum samples by the standard addition method and the recovery value for glucose ranged from 94 to 113% (Table 1).

The proposed biosensor exhibited a wide linear range and a low detection limit if compared to the performance of other electrodes proposed for the determination of H_2O_2 [2,28,48,49], as illustrated in Table 2.

Table 1
Determination of hydrogen peroxide in synthetic human plasma.

Sample	Added (10^{-6} mol L^{-1})	Proposed electrode (10^{-6} mol L^{-1})	Recovery (%)
A	9.10	10.3	113
B	38.5	36.1	94
C	65.5	65.0	99

Table 2
Comparison of the analytical data between the present work and some recently reported biosensors for hydrogen peroxide determination.

Biosensor	Linear range (mol L^{-1})	Detection limit (mol L^{-1})	Reference
Myoglobin–AgNPs–CNTs	$2.0 \times 10^{-6} - 1.2 \times 10^{-3}$	3.6×10^{-7}	Liu et al. [48]
Peroxidase–AgNPs/DNA-functionalized	$1.5 \times 10^{-6} - 2.0 \times 10^{-3}$	5.0×10^{-7}	Wang et al. [28]
Hb–graphene–Fe_3O_4/GCE	$2.3 \times 10^{-6} - 9.6 \times 10^{-3}$	1.1×10^{-6}	Wang et al. [2]
Hb–CTS/nano-$CaCO_3$/GCE	$3.7 \times 10^{-5} - 8.3 \times 10^{-4}$	8.3×10^{-6}	Shan et al. [50]
Hb–CNTs	$2.1 \times 10^{-4} - 9.0 \times 10^{-4}$	9.0×10^{-6}	Zhao et al. [49]
Hb–AgNPs–PAMAM/GCE	$6.0 \times 10^{-6} - 9.1 \times 10^{-5}$	4.9×10^{-6}	This work

CNTs: multi-walled carbon nanotubes.
CTS: chitosan.

4. Conclusions

An electrochemical biosensor was developed upon modification of a glassy carbon electrode with Hb, AgNPs and PAMAM. The Hb molecules immobilized in conjunction with AgNPs–PAMAM exhibited good biological activity forming a stable and uniform bioreceptor layer. The system was successfully applied to the determination of H_2O_2 over the linear range from 6.0×10^{-6} to 9.1×10^{-5} mol L^{-1} with the detection limit of 4.9×10^{-6} mol L^{-1}. Therefore, we suggest that films containing AgNPs and PAMAM are attractive to use in sensing and biosensing.

Acknowledgments

We would like to thank FAPESP (12/02877-4), CNPq (441428/2014-2) and CAPES for the financial support.

References

[1] J.Y. Sun, K.J. Huang, S.F. Zhao, Y. Fan, Z.W. Wu, Bioelectrochemistry 82 (2011) 125–130.
[2] Y.Q. Wang, H.J. Zhang, D. Yao, J.J. Pu, Y. Zhang, X.R. Gao, Y.M. Sun, J. Solid State Electrochem. 17 (2013) 881–887.
[3] C.X. Cai, J. Chen, Anal. Biochem. 325 (2004) 285–292.
[4] Y. Zhang, H.M. Cao, W.W. Fei, D.X. Cui, N.Q. Jia, Sens. Actuators, B 162 (2012) 143–148.
[5] H.F. Xu, H. Dai, G.N. Chen, Talanta 81 (2010) 334–338.
[6] X. Luo, A. Morrin, A.J. Killard, M.R. Smyth, Electroanalysis 18 (2006) 319–326.
[7] C.A. Mirkin, Small 1 (2005) 14–16.
[8] B.C. Janegitz, L.H. Marcolino-Junior, S.P. Campana-Filho, R.C. Faria, O. Fatibello-Filho, Sens. Actuators, B 142 (2009) 260–266.
[9] G.G. Oliveira, B.C. Janegitz, V. Zucolotto, O. Fatibello-Filho, Cent. Eur. J. Chem. 11 (2013) 1837–1843.
[10] H.H. Takeda, B.C. Janegitz, R.A. Medeiros, L.H.C. Mattoso, O. Fatibello-Filho, Sens. Actuators, B 161 (2012) 755–760.
[11] B.C. Janegitz, L.C.S. Figueiredo-Filho, L.H. Marcolino-Junior, S.P.N. Souza, E.R. Pereira-Filho, O. Fatibello-Filho, J. Electroanal. Chem. 660 (2011) 209–216.
[12] F.C. Vicentini, A. Elisa Ravanini, T.A. Silva, B.C. Janegitz, V. Zucolotto, O. Fatibello-Filho, Analyst 139 (2014) 3961–3967.
[13] X. Gan, T. Liu, X.L. Zhu, G.X. Li, Anal. Sci. 20 (2004) 1271–1275.
[14] P. Raghu, T.M. Reddy, K. Reddaiah, L. Jaidev, G. Narasimha, Enzym. Microb. Technol. 52 (2013) 377–385.
[15] F.C. Vicentini, B.C. Janegitz, C.M.A. Brett, O. Fatibello-Filho, Sensors Actuators B Chem. 188 (2013) 1101–1108.
[16] B.C. Janegitz, J. Cancino, V. Zucolotto, J. Nanosci. Nanotechnol. 14 (2014) 378–389.
[17] C. Shan, H. Yang, D. Han, Q. Zhang, A. Ivaska, L. Niu, Biosens. Bioelectron. 25 (2010) 1070–1074.
[18] L.C.S. Figueiredo-Filho, T.A. Silva, F.C. Vicentini, O. Fatibello-Filho, Analyst 139 (2014) 2842–2849.
[19] Y. Zhang, G.M. Zeng, L. Tang, D.L. Huang, X.Y. Jiang, Y.N. Chen, Biosens. Bioelectron. 22 (2007) 2121–2126.
[20] L. Tang, G.M. Zeng, G.L. Shen, Y. Zhang, Y.P. Li, C.Z. Fan, C. Liu, C.G. Niu, Anal. Bioanal. Chem. 393 (2009) 1677–1684.
[21] B.C. Janegitz, R.A. Medeiros, R.C. Rocha-Filho, O. Fatibello-Filho, Diam. Relat. Mater. 25 (2012) 128–133.
[22] J. Zhang, Y. Sun, B. Xu, H. Zhang, Y. Gao, H. Zhang, D. Song, Biosens. Bioelectron. 45 (2013) 230–236.
[23] X.C. Tan, M.J. Li, P.X. Cai, L.J. Luo, X.Y. Zou, Anal. Biochem. 337 (2005) 111–120.
[24] G.G. Oliveira, D.C. Azzi, F.C. Vicentini, E.R. Sartori, O. Fatibello-Filho, J. Electroanal. Chem. 708 (2013) 73–79.
[25] F.W. Campbell, R.G. Compton, Anal. Bioanal. Chem. 396 (2010) 241–259.
[26] E. Navarro, F. Piccapietra, B. Wagner, F. Marconi, R. Kaegi, N. Odzak, L. Sigg, R. Behra, Environ. Sci. Technol. 42 (2008) 8959–8964.
[27] J.-Z. Xu, Y. Zhang, G.-X. Li, J.-J. Zhu, Mater. Sci. Eng. C 24 (2004) 833–836.
[28] F. Wang, R. Yuan, Y. Chai, D. Tang, Anal. Bioanal. Chem. 387 (2007) 709–717.
[29] R. Rawal, S. Chawla, C.S. Pundir, Anal. Biochem. 419 (2011) 196–204.
[30] N.T. Pourianazar, P. Mutlu, U. Gunduz, J. Nanoparticle Res. 16 (2014).
[31] K. Sadler, J.P. Tam, Rev. Mol. Biotechnol. 90 (2002) 195–229.
[32] X. Li, Y. Wang, X. Sun, T. Zhan, W. Sun, J. Chem. Sci. 122 (2010) 271–278.
[33] X.M. Liu, X.Y. Zhang, Y.L. Zhao, W.L. Liu, B.J. Wang, Y.H. Zhang, Z.Q. Zhang, Chem. Res. Chin. Univ. 26 (2010) 723–728.
[34] H.Y. Gu, A.M. Yu, H.Y. Chen, J. Electroanal. Chem. 516 (2001) 119–126.
[35] S.R. Bhatia, S.F. Khattak, S.C. Roberts, Curr. Opin. Colloid Interface Sci. 10 (2005) 45–51.
[36] M.F. Perutz, A. Wilkinson, M. Paoli, G. Dodson, Annu. Rev. Biophys. Biomol. Struct. 27 (1998) 1–34.
[37] A.J. Bard, L.R. Faulkner, Electrochemical Methods: Fundamentals and Applications, 2 ed. John Wiley & Sons, New York, 2001.
[38] S. Niu, B. Han, W. Cao, S. Zhang, Anal. Chim. Acta 651 (2009) 42–47.
[39] J.W. Li, L.H. Liu, F. Xiao, Z. Gui, R. Yan, F.Q. Zhao, L. Hu, B.Z. Zeng, J. Electroanal. Chem. 613 (2008) 51–57.
[40] Q.Q. Guo, S.J. Ji, Q.L. Yue, L. Wang, J.F. Liu, J.B. Jia, Anal. Chem. 81 (2009) 5381–5389.
[41] B. Royo, M. Sosna, A.C. Asensio, J.F. Moran, E.E. Ferapontova, J. Electroanal. Chem. 704 (2013) 67–74.
[42] E. Laviron, J. Electroanal. Chem. 101 (1979) 19–28.
[43] X. Feng, R. Li, C. Hu, W. Hou, J. Electroanal. Chem. 657 (2011) 28–33.
[44] E.A. Veal, A.M. Day, B.A. Morgan, Mol. Cell 26 (2007) 1–14.
[45] O. Fatibello-Filho, M.D. Capelato, Quim. Nova 15 (1992) 28–39.
[46] L. Gorton, E. Csöregi, E. Dominguez, J. Emneus, G. Jönsson-Pettersson, G. Marko-Varga, B. Persson, Anal. Chim. Acta 250 (1991) 203–248.
[47] L. Tian, Y. Feng, Y. Qi, B. Wang, Y. Chen, X. Fu, Microchim. Acta 177 (2012) 39–45.
[48] C.-Y. Liu, J.-M. Hu, Biosens. Bioelectron. 24 (2009) 2149–2154.
[49] Y.-D. Zhao, Y.-H. Bi, W.-D. Zhang, Q.-M. Luo, Talanta 65 (2005) 489–494.
[50] D. Shan, S. Wang, H. Xue, S. Cosnier, Electrochem. Commun. 9 (2007) 529–534.